Cytokine 113 (2019) 144–154

Contents lists available at ScienceDirect

Cytokine

journal homepage: www.elsevier.com/locate/cytokine

Interleukin 29 inhibits RANKL-induced osteoclastogenesis via activation of JNK and STAT, and inhibition of NF-κB and NFATc1

Qiuyue Peng[a,1,2], Aishu Luo[b,1], Zihao Zhou[c], Wenhua Xuan[b], Ming Qiu[c], Qin Wu[b], Lingxiao Xu[b], Xiangqing Kong[c], Miaojia Zhang[b], Wenfeng Tan[b,d,*], Meilang Xue[e], Fang Wang[c,*]

[a] Department of Traditional Chinese Medicine, The First Affiliated Hospital of Nanjing Medical University, Nanjing 210029, China
[b] Department of Rheumatology, The First Affiliated Hospital of Nanjing Medical University, Nanjing 210029, China
[c] Department of Cardiology, The First Affiliated Hospital of Nanjing Medical University, Nanjing 210029, China
[d] Institute of Integration of Traditional Chinese and Western Medicine, Nanjing Medicine University, Nanjing 211166, China
[e] Sutton Arthritis Research Laboratories, The University of Sydney at Royal North Shore Hospital, Sydney, NSW 2065, Australia

ARTICLE INFO

Keywords:
Interleukin 29
Osteoclast
RANKL
NFATC1
STAT

ABSTRACT

Interleukin (IL)-29 is known to modulate immune functions of monocytes or macrophages. In this study, we investigated the effect and its underlying mechanism of IL-29 on receptor activator of nuclear factor κB ligand (RANKL)-induced osteoclastogenesis using murine macrophage cell line RAW264.7 cells and bone-marrow-derived monocyte/macrophage precursor cells (BMMs), and human peripheral blood mononuclear cells (PBMCs). In response to human recombinant IL-29, cell viability and apoptosis were assessed by Cell Counting Kit-8 and flow cytometry; the osteoclast formation and activity by tartrate-resistant acid phosphatase (TRAP) staining and pit formation assay, respectively; the expression and activation of molecules that associated with osteoclastogenesis by real time-PCR, immunoblotting or immunofluorescent analysis. IL-28 receptor α (IL-28Rα), a specific receptor of IL-29 was expressed on RAW264.7 cells. Although IL-29 did not affect the viability and apoptosis of RAW264.7 cells, it inhibited multinucleated cells in the differentiation of osteoclastogenesis, the bone-resorbing activity of mature osteoclasts and osteoclastic specific genes expression including TRAP, cathepsin K (CTSK), nuclear factor of activated T-cells, cytoplasmic 1 (NFATc1), C-Fos and matrix metallopeptidase 9 (MMP-9). This inhibitory effect of IL-29 was confirmed on BMMs and PBMCs and mediated via IL-28Rα through the activation of Stat1 and 3 and the suppression of nuclear factor kappa B (NF-κB) and NFATc1 nuclear translocation in RAW264.7 cells. In conclusion, IL-29 inhibited osteoclastogenesis via activation of STAT signaling pathway, prevention of NF-κB activation and NFATc1 translocation, and suppression of downstream osteoclastogenic genes expression.

1. Introduction

Interleukin (IL)-29 is a new member of the recently discovered interferon (IFN) λ family, together withIL-28A and IL-28B, comprising the Type III IFNs, also labeled as IFNλ1, IFNλ2 and IFNλ3, respectively [1–3]. IL-29 is the most potent and abundant cytokine of IFNλs in humans, despite only existing as a pseudogene in mice [4]. IL-29 binds to the complex receptor comprised the shared IL-10R2 (IL-10Rβ), and the IFN-λ-specific IFN-λR1 (IL-28 receptor α, IL-28Rα) chain. IL-28Ra is widely expressed by ranges of cells including epithelial cells, hepatocytes, fibroblasts [5,6], and immune cells, such as human peripheral blood plasmacytoid DCs, monocytes, B cells [7,8], and NK cells [9].

IL-29 possesses antiviral and immune regulation properties [2,10–12]. In recent years, IL-29 has also been found involving in the pathogenesis of a variety of immune diseases, such as systemic lupus erythematosus (SLE) [13,14], asthma [7], psoriasis [15], and Sjögren's syndrome[16], as well as a variety of cancers including skin cancer, lung cancer, esophageal carcinomas, hepatocellular carcinomas and

Abbreviations: IL-29, Interleukin-29; IL-28Rα, IL-28 receptor α; RANKL, receptor activator of nuclear factor κB ligand; M-CSF, macrophage colony-stimulating factor; TRAP, tartrate-resistant acid phosphatase; NFATc1, nuclear factor of activated T-cells, cytoplasmic 1; MMP-9, matrix metallopeptidase 9; NF-κB, nuclear factor kappa B; RA, rheumatoid arthritis; BMM, bone-marrow-derived monocyte/macrophage precursor cells

* Corresponding authors at: Department of Rheumatology, The First Affiliated Hospital of Nanjing Medical University, Nanjing 210029, China (W. Tan).
E-mail addresses: tw2006@njmu.edu.cn (W. Tan), wangfangheart@njmu.edu.cn (F. Wang).

[1] Qiuyue Peng and Aishu Luo contributed equally to this work.

[2] Present address: Emergency Department, Traditional Chinese Medical Hospital of Hubei Province, Wuhan 430000, China.

https://doi.org/10.1016/j.cyto.2018.06.032
Received 25 October 2017; Received in revised form 14 June 2018; Accepted 29 June 2018
Available online 09 July 2018

gastric cancer [4]. We have demonstrated that IL-29 is dysregulated in patients with rheumatoid arthritis (RA) and contributes to RA pathogenesis via promoting proinflammatory cytokines, chemokines or matrix metalloproteinases (MMPs) production in synovial fibroblasts [5,17], as well as stimulating inflammation and cartilage degradation in osteoarthritis [6]. However, the role of IL-29 in bone resorption is unclear.

Bone is a dynamic organ that continuously undergoes remodeling involving osteoclastic bone resorption and osteoblastic bone formation. The enhanced osteoclastic bone resorption causes severe bone damage leading to progressive joint destruction as seen in osteoclast-related disorders, such as RA [18]. Osteoclasts originate from the hematopoietic stem cells and develop through the fusion of mononuclear myeloid precursors. Mature osteoclasts are large, multinucleated cells located on trabecular and endosteal cortical bone surfaces. A variety of factors, including tumor necrosis factor (TNF) superfamily ligands and inflammatory proteins from different cell sources, contribute to the formation and function of osteoclasts. The differentiation of osteoclasts is induced by two crucial cytokines: macrophage colony-stimulating factor (M-CSF), which regulates the proliferation and survival of osteoclast precursors [19], and RANKL, which stimulates the differentiation of osteoclast precursors into mature osteoclasts [20,21].

Of note, osteoclastogenesis occurs in the RA synovial tissue when osteoclast precursors are exposed to M-CSF and RANKL. Bone erosion in RA is associated with increased production of pro-inflammatory cytokines and accelerated osteoclastogenesis in affected joints [22]. Proinflammatory cytokines that accumulated in inflammatory joint of RA, such as TNF-α, IL-1β, IL-6, IL-15 and IL-17 promote osteoclastogenesis and bone resorption through multiple mechanisms including increase of the production of M-CSF and RANKL [22,23], whereas cytokines IL-33, IL-12 and IL-23, as well as the type I and type II IFNs, are potent suppressors of osteoclastogenesis [18,23–25]. Although these factors are also expressed in RA synovial tissue, their actions cannot outweigh the bone-resorptive effects within RA synovium [22].

IL-29 is an important proinflammatory cytokine in RA [5,17], however, its effect and role in osteoclastogenesis in RA remains unknown. To address this issue, we investigated the potential role of IL-29 in the osteoclasts formation *in vitro* and demonstrated a marked inhibitory effect of IL-29 on osteoclast formation in RANKL-stimulated RAW264.7 cells and bone-marrow-derived monocyte/macrophage precursor cells (BMMs).

2. Materials and methods

2.1. Cell line and reagents

Murine RAW264.7 cells were obtained from ATCC; recombinant human IL-29, human and murine soluble RANK Ligand & M-CSF from Peprotech (Rocky Hill, NJ, USA); rabbit anti-mouse IL-28Rα polyclonal antibody from Abcam (Cambridge, MA, USA); phospho-Stat antibody sampler kit, cellular activation of signaling kits for c-Jun N-terminal kinase (JNK), extracellular signal-regulated kinase (ERK), p38, and primary antibody for NFκBp65 and NFATc1 from Cell Signaling Technology (Beverly, MA, USA); Osteo Assay Surface from Corning (Lowell, MA, USA); Annexin V/PI Apoptosis Detection Kit from Vazyme Biotech (Nanjing, China); Alexa Flor^R 647 donkey anti-rabbit IgG, Alexa Fluor^{R}488 donkey anti-goat IgG from Biolegend (San Diego, CA, USA) and a cell fixation and permeabilization kit from eBioscience (San Diego, CA, USA); Leukocyte Acid Phosphatase Assay kit from Sigma (St. Louis, USA); M-PER buffer or NE-PER Nuclear and Cytoplasmic Extraction Reagents (Thermo). Tissue culture reagents including Dulbecco's modified Eagle's medium (DMEM), a-minimal essential medium (α-MEM) and fetal bovine serum (FBS) from Gibco (Carlsbad, CA, USA).

2.2. Cell culture and osteoclast differentiation

RAW264.7 cells were cultured in DMEM containing 10% heat-inactivated fetal bovine serum (FBS), penicillin (100 U/ml) and streptomycin (100 μg/ml) in a humidified atmosphere with 5% CO_2 at 37 °C. To induce osteoclast differentiation, RAW264.7 cells suspended in α-MEM with 10% FBS, 100 U/ml penicillin and 100 μg/ml streptomycin were seeded in a 96-well plate in triplicate and cultured with IL-29 (0, 1, 10 and 100 ng/ml) and 50 ng/ml murine soluble RANKL for 5 days. All media were replaced every 3 days.

Primary bone marrow cells were isolated from 8-week-old C57/BL6 mice by flushing femurs and tibias and cultured with M-CSF (100 ng/ml) on peri dishes in α -MEM with 10% FBS, 100 U/ml penicillin, 100 μg/ml streptomycin. After 2 days, floating cells were discarded and adherent cells (BMMs) were seeded in a 96-well plate in triplicate, treated with different concentrations of IL-29 (0, 1, 10 and 100 ng/ml) plus M-CSF (60 ng/ml) and murine soluble RANKL (100 ng/ml) in a-MEM containing 10% FBS for 7 days. All differentiated media were replaced every 3 days.

Human peripheral blood mononuclear cells (PBMCs) were isolated from healthy donors by Ficoll-Hypaque density centrifugation. After washing twice, PBMCs were incubated with 100 ng/ml of M-CSF for 2 days in α-MEM supplemented with 10% FBS to generate monocyte-derived osteoclast precursors (OCPs). For human osteoclastogenesis assay, OCPs were added to 48-well plate in triplicate at a seeding density of 1.5×10^6 cells per well, and incubated with IL-29 (0, 1, 10 and 100 ng/ml) in the presence of M-CSF (60 ng/ml) and human RANKL (100 ng/ml) for 14 additional days in a-MEM containing 10% FBS, with exchange of differentiated media every 3 days.

2.3. Cell proliferation assay

To examine cell proliferation, a Cell Counting Kit-8 was used according to the manufacturer's instructions. RAW264.7 cells were seeded at a density of 5×10^3 cells/well in a 96-well plate for 24 h, then cells were treated with IL-29 (0, 1, 10, 100 ng/ml). After another 72 h, the culture medium was replaced by the medium containing 10 μl CCK-8 and cells were incubated at 37 °C for an additional 4 h. The absorbance was then measured at a wavelength of 450 nm on a microplate reader (Bio-Tek, Vermont, USA).

2.4. Apoptosis assay

RAW264.7 cells were treated with IL-29 (0, 1, 10 and 100 ng/ml) in the presence of murine RANKL (50 ng/ml). After 48 h, cells were harvested and stained with the Annexin V-FITC Apoptosis Detection Kit according to the manufacturer's instructions. In brief, after washing twice with phosphate buffer saline (PBS), cells were suspended in100 μl Annexin V binding buffer and incubated with 5 μl Annexin V-FITC and 5 μl propidium iodide (PI) staining solution for 15 min at room temperature away from light before addition of 400 μl Annexin V binding buffer. Finally, cells were analyzed by a FACSCalibur Flow cytometer (BD Biosciences, San Jose, CA).

2.5. Tartrate-resistant acid phosphatase staining

Cells were washed with PBS and fixed with 4% paraformaldehyde for 30 min. After washing with PBS, cells were incubated at 37 °C in the dark for 1 h in the reaction mixture of the Leukocyte Acid Phosphatase Assay kit, as directed by the manufacturer. Cells were then washed three times with distilled water and TRAP positive multinucleated cells containing three or more nuclei were photographed and counted under a light microscope with a 10× objective (Nikon, Japan).

Table 1
Mouse primers used for real-time quantitative PCR.

Gene Symbol	Forward (5′-3′)	Reverse (5′-3′)
TRAP	CCAATGCCAAAGAGATCGCC	TCTGTGCAGAGACGTTGCCAAG
CTSK	GACGCAGCGATGCTAACTAA	CCAGCACAGAGTCCACAACT
NFATc1	GGAGAGTCCGAGAATCGAGAT	TTGCAGCTAGGAAGTACGTCT
C-Fos	ATGATGTTCTCGGGTTTCAACG	CAGTCTGCTGCATAGAAGGAACCG
MMP-9	CTGGACAGCCAGACACTAAAG	CTCGCGGCAAGTCTTCAGAG
18S	TCAAGAACGAAAGTCGGAGG	GGACATCTAAGGGCATCAC

2.6. Pit formation assay

Resorption pit formation assay was performed using the Osteo Assay kit (Cat.3988; Corning, WA, USA). In brief, RAW264.7 cells were seeded into a 24-well plate and incubated withIL-29 (0, 1, 10 and 100 ng/ml) and murine RANKL (50 ng/ml) for 5 days. After three washes, resorption pits on the plate were visualized under a light microscope (Nikon, Japan). The ratio of the resorbed area to the total area was measured in four optical fields on a slice using Image-Pro Plus version4.0 (Media Cybernetics, Inc., Rockville, MD, USA).

2.7. Real time PCR assay

Total RNA was isolated from RAW264.7 cells using TRIzol reagent (Invitrogen) and reverse transcribed using PrimeScript™RT MasterMix (Takara) according to the manufacturer's instructions. Quantitative real-time PCR was performed on Applied Biosystems 7900HT Instrument (Applied Biosystems, CA, USA) as we described previously [5]. The primer sequences were shown in Table 1. All samples were assayed in triplicate. Relative gene expression was determined by the $2^{-\Delta\Delta Ct}$ method.

2.8. Flow cytometric analysis

IL-28Rα expression on cell surface was assessed using flow cytometric analysis according to a previously published protocol [6]. Briefly, RAW264.7 cells (1×10^6) were harvested, and blocked with 1% bovine serum albumin (BSA) for 30 min, stained with IL-28Rα antibody for 25 min at room temperature, and washed twice with PBS. Then cells were incubated with Alexa Fluor^{R}488 donkey anti-goat IgG at room temperature in the dark for 25 min before analyzed on a FACSCalibur Flow cytometer (BD Biosciences, San Jose, CA, USA). For detection of NFATc1 in cell nuclear, after incubation with IL-29 (100 ng/ml) in the presence of murine RANKL (50 ng/ml) for 48 h, RAW264.7 cells were trypsinized, washed twice with PBS, then fixed and permeabilized using a cell fixation and permeabilization kit (eBioscience) and then stained and analyzed as described above for IL-28Rα.

2.9. Adenovirus vectors construction and transfection in RAW264.7 cells

Adenovirus vectors encoding shRNAs against mouse IL-28Rα and scrambled shRNA controls were designed and manufactured by Obio Technology Co., Ltd (Shanghai, China). RAW264.7 cells in α-MEM containing 10% FBS and 1% penicillin-streptomycin were planted in 24-well plates to 60–70% confluency and cultured for 24 h. Then cells were transfected with recombinant adenovirus expressing IL-28Rα shRNA or scrambled GFP control for 48 h. Cells were further cultured in growth media with murine RANKL (50 ng/ml) and IL-29 (100 ng/ml) for 5 days to induce osteoclast differentiation. Finally cells were stained for TRAP and Leukocyte Acid Phosphatase Assay kit.

2.10. Western blot assay

Proteins were extracted with M-PER buffer or NE-PER Nuclear and Cytoplasmic Extraction Reagents (Thermo Fisher Scientific Inc, Rockford, USA) according to the manufacturer's protocol. Equivalent amounts of protein were loaded for sodium dodecyl sulfate-polyacrylamide gel electrophoresis (SDS-PAGE), and immunoblotting was performed using specific antibodies for p38, phosphor (p)-p38, ERK, p-ERK, c-Jun N-terminal kinase (JNK), p-JNK, Stat1/2/3//4/5/6, pStat1/2/3//4/5/6, NF-κBp65, NFATc1, GAPDH and H3. The signals were visualized with Super Signal West Dura chemiluminescent detection reagents following the manufacturer's directions (Thermo Fisher Scientific), and protein bands were scanned and semi-quantified with the Gel-pro Analyzer software (Bio-Rad, CA, USA). GAPDH and H3 were used as an internal protein loading controls.

2.11. Immunofluorescent staining

RAW264.7 cells were seeded onto glass coverslips and then incubated with IL-29 (100 ng/ml) and murine RANKL (50 ng/ml). After 48 h stimulation, the distribution and expression of NFATc1 protein was assessed according to previously published protocols [5]. Briefly, cells were washed in PBS, fixed in 4% paraformaldehyde, permeabilized with 0.3% Triton X-100, blocked with 5% BSA and incubated with a specific anti-NFATc1monoclonal antibody at 4 °C overnight. After washing, cells were further incubated for 1 h with FITC-conjugated goat anti-mouse IgG at room temperature. Finally, cells were nuclear-stained with DAPI, and fluorescence was visualized using a Zeiss fluorescence microscope (Axio Vert.A1, Oberkochen, Germany). NFATc1wasstained with green and nuclei were stained with blue. The nuclear localization of NFATc1 was confirmed in merged images (cyan). IL-28Rα distribution and expression in RAW264.7 cells was also examined following previously published protocols [5].

2.12. Statistical analysis

All data were analyzed using GraphPad Prism 6.0 software (GraphPad Software, La Jolla, CA, USA) and SPSS software (SPSS, Inc, Chicago, IL, USA), and expressed as mean ± SEM. Differences between two groups were performed with Student's *t* test for parametric data and Mann-Whitney *U* test for nonparametric data. A *P*-value of < 0.05 was considered as a significant difference.

3. Results

3.1. IL-28Rα expression in RAW264.7 cells and effects of IL-29 on survival of osteoclast precursors

To examine whether osteoclast precursors express IL-28Ra, a specific receptor of IL-29, osteoclast precursor cell line RAW264.7 was stained for IL-28Ra and analyzed by the immunofluorescent microscope and flow cytometry. As shown in Fig. 1A and B, RAW264.7 cells expressed high levels of IL-28Ra, suggesting that these cells may respond to IL-29 stimulation.

The survival of osteoclast precursors is very important for osteoclast formation. Thus, we examined the effect of IL-29 on cell viability and apoptosis in RANKL-induced osteoclastogenesis. RAW264.7 cells were treated with various concentrations of IL-29, cell viability was measured by a CCK8 assay and apoptosis by flow cytometry. IL-29 affected neither cell viability after 72 h treatment even at the high dose 100 ng/ml IL-29 (Fig. 1C), nor cell apoptosis after 48 h stimulation (Fig. 1D). Taken together, these data suggests that IL-29 does not affect osteoclast precursors survival.

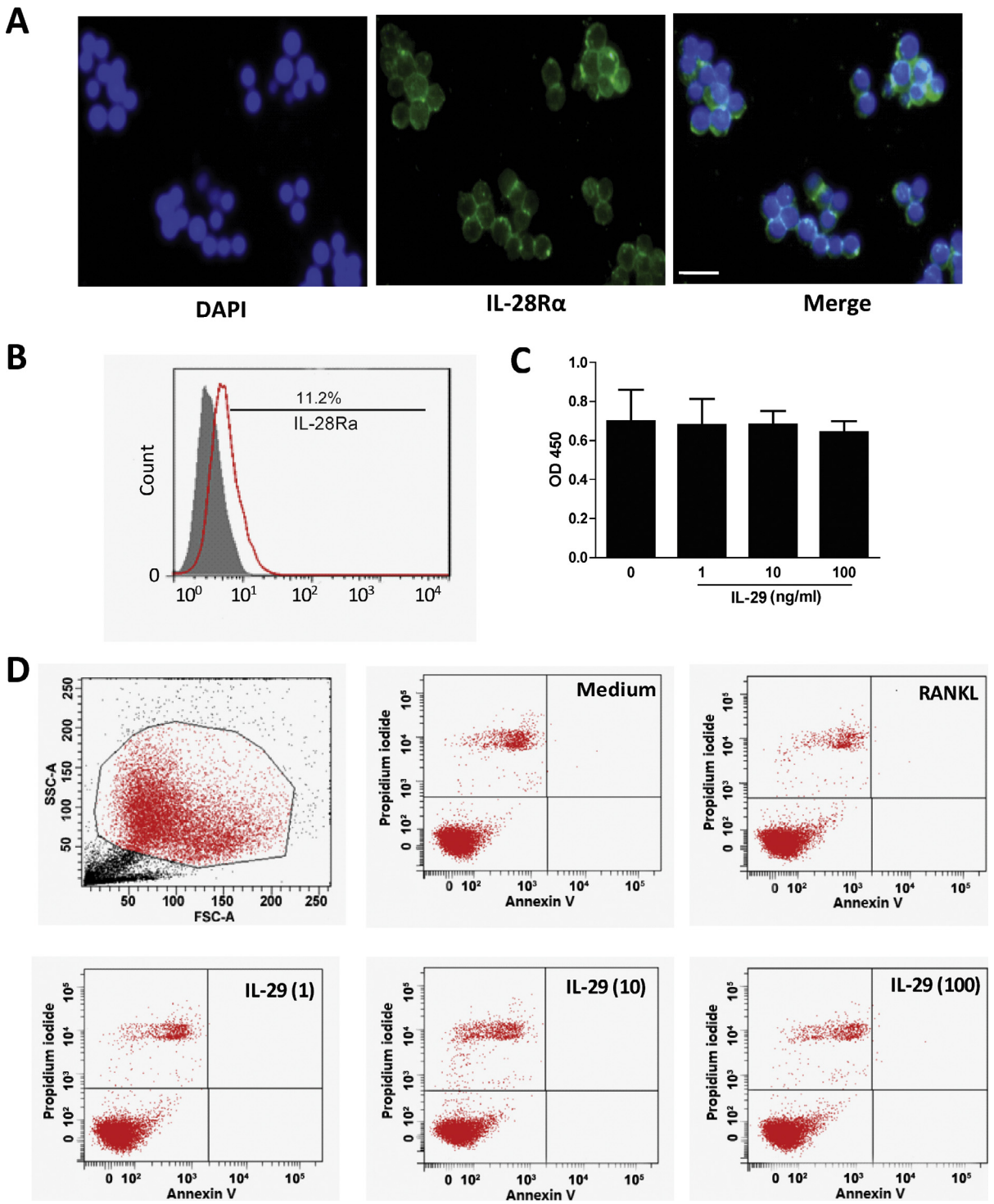

Fig. 1. Effect of IL-29 on survival of RANKL-stimulated RAW264.7 cells. The expression of IL-28Rα in RAW264.7 cells, detected by immunofluorescent staining (A) and flow cytometry (B), the gray peak in B represents a negative control. (C) RAW264.7 cells viability after being incubated with IL-29 at 1, 10, and 100 ng/ml for 72 h, measured by CCK-8 assay. (D) RAW264.7 cells apoptosis after treated with IL-29 (1, 10 and 100 ng/ml) in the presence of RANKL (50 ng/ml) for 48 h, detected by Annexin V apoptosis assay. Scale bar: 50 μM. Medium: medium used for RAW264.7 cells treatment.

3.2. Effects of IL-29 on RANKL-induced osteoclast differentiation

We next investigated the effect of IL-29 on osteoclast differentiation in RAW264.7 cells using TRAP, a specific marker of osteoclast differentiation. IL-29 alone had no effect on osteoclast formation (data not shown). In the presence of RANKL, IL-29 decreased the number of multinucleated osteoclasts in a dose-dependent manner (Fig. 2A). This effect was further confirmed in primary BMMs and human PBMCs. BMMs were cultured in the presence of M-CSF (60 ng/ml) and RANKL (100 ng/ml) together with IL-29 (1, 10 and 100 ng/ml) for 7 days. IL-29 dose-dependently reduced the number of TRAP-positive multinucleated cells, with significant suppression (about 60%, 70% respectively) occurring at 10 and 100 ng/ml (Fig. 2B). Considering that IL-29 is not expressed in mice, we further investigated this effect in human PBMCs. Similarly, IL-29 suppressed the differentiation of human OCPs into mature osteoclasts induced by M-CSF (60 ng/ml) and RANKL (100 ng/

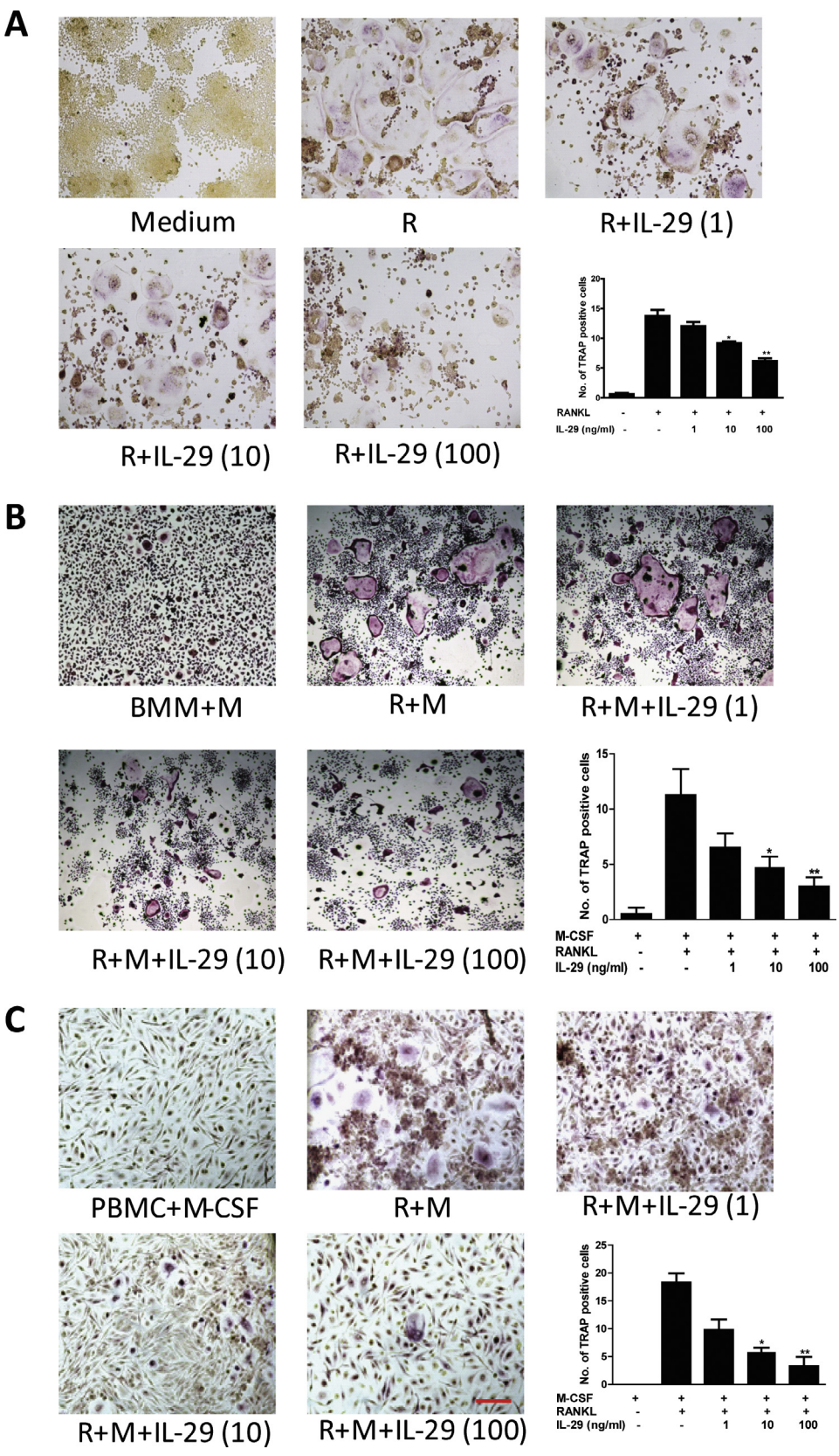

Fig. 2. Effect of IL-29 on RANKL-induced osteoclast differentiation of RAW264.7, BMMs and human PBMCs. (A) TRAP staining in RAW264.7 cells after treated with IL-29 (0, 1, 10 and 100 ng/ml) in the presence of RANKL (50 ng/ml) for 5 days. (B) TRAP staining in BMMs after treated with IL-29 (0, 1, 10 and 100 ng/ml) as well as RANKL (100 ng/ml) and M-CSF (60 ng/ml) for 7 days. (C) TRAP staining in human PBMC after treated with IL-29 (0, 1, 10 and 100 ng/ml) in the presence of RANKL (100 ng/ml) and M-CSF (60 ng/ml) for 14 days. At the end of the culture, cells were washed and stained with TRAP. The TRAP positive multinucleated (more than three nuclei) cells were counted in triplicate. The figures represent one of three independent experiments. Data are expressed as mean ± SEM (n = 3). $^{*}P < 0.05$ and $^{**}P < 0.01$ vs RANKL-treated group. M: M-CSF; R: RANKL; Medium: medium used for RAW264.7 cells treatment. Scale bar: 50 μM.

ml) in a dose dependent manner, assessed by TRAP staining (Fig. 2C). Collectively, our results showed that IL-29 inhibited RANKL-induced osteoclast formation.

3.3. Effects of IL-29 on bone resorption in cell cultures

To investigate the effect of IL-29 on osteoclastic bone resorption, resorption pit formation was performed. RAW264.7 cells were plated into a 24-well plate and treated with IL-29 (0, 1, 10 and 100 ng/ml) in

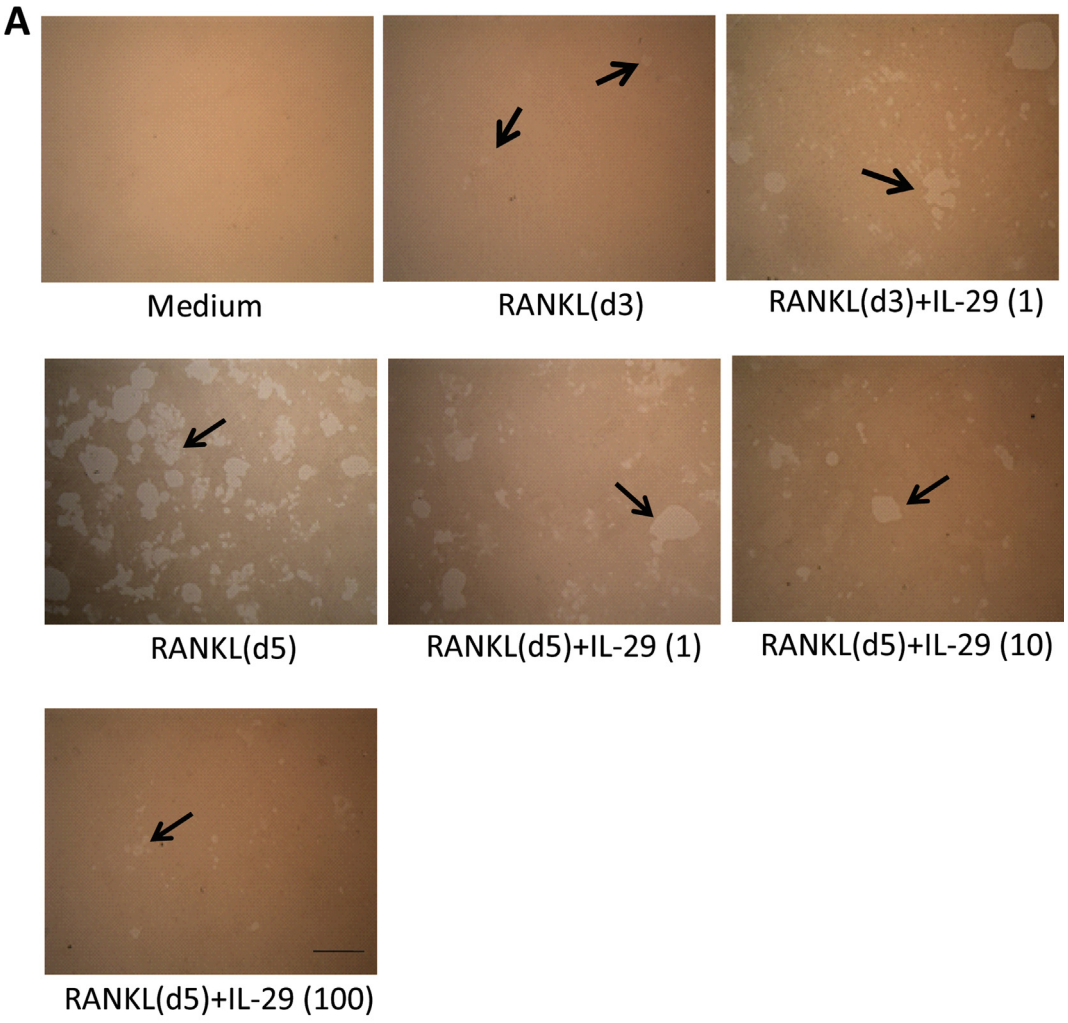

Fig. 3. Effect of IL-29 on resorption pit formation. (A) The resorption pit formation of RAW264.7 cells. Cell were seeded into a 24-well plate (Osteo Assay Kit) and pretreated with 50 ng/ml RANKL for 3 days (RANKL d3), then cells were removed from the culture or with IL-29 (100 ng/ml) for additional 2 days in the presence of RANKL (50 ng/ml), or cells were treated with IL-29 (0, 1, 10 and 100 ng/ml) in the presence or absence of RANKL 50 ng/ml) for 5 days (RANKL d5). After the incubation, the cells were washed and removed from the culture, and the wells were photographed to visualize resorption pits. Arrows indicate pit area. (B) Percentage of resorbed area was determined using the Image software, and the percentage resorption generated by RANKL alone is set as 100%. Scale bar: 50 μM. Data are expressed as mean ± SEM from three slices. The figures represent one of three independent experiments. $^{*}P < 0.05$ and $^{**}P < 0.01$ vs RANKL-treated group for 5 days (RANKL 5d), $^{\#\#}P < 0.01$ vs RANKL-treated group for 3 days (RANKL 3d). Medium: medium used for RAW264.7 cells treatment.

the presence of RANKL (50 ng/ml). After 5 days, many resorption pits were formed in the stimulation of RANKL. IL-29 reduced RANKL-stimulated bone resorption area approximately 65–85% in a dose dependent manner (Fig. 3), indicating that IL-29 represses osteoclast function by inhibiting osteoclastogenesis.

To assess the effect of IL-29 for the suppression of mature resorbing osteoclasts, RAW264.7 cells were treated with murine RANKL (50 ng/ml) for 3 days, then IL-29 (100 ng/ml) was added for additional 2 days.

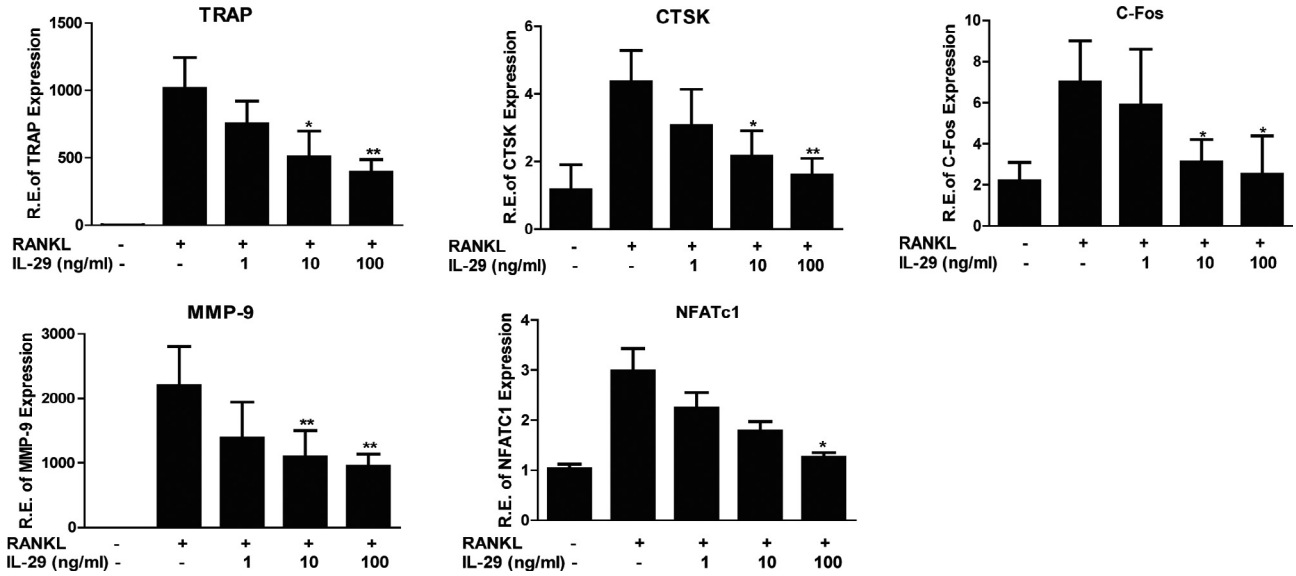

Fig. 4. Effect of IL-29 on osteoclastogenic mRNA expression. mRNA levels of TRAP, CTSK, NFATc1, C-Fos and MMP-9 in RAW264.7 cells treated with 100 ng/ml IL-29 in the presence of RANKL (50 ng/ml) for 5 days and determined by real time PCR. Data are expressed as mean ± SEM (n = 3). A representative image of three independent experiments was shown. $^{*}P < 0.05$ and $^{**}P < 0.01$ vs RANKL-treated group.

Surprisingly, few osteoclasts was observed after RANKL stimulation alone for 3 days, IL-29 additional 2 days treatment notably increased the resorbing area (about 7.4 fold change) (Fig. 3). This is consistent with the data showing that IL-29 decreased around 65–85% resorption area when compared to RANKL induction alone for 5 days (Fig. 3). Our results collectively indicate that IL-29 exhibits the inhibitory action on osteoclastogenesis mostly by suppression of osteoclasts differentiation rather than mature osteoclasts activity.

3.4. Effect of IL-29 on osteoclastogenic genes expression

TRAP, CTSK, MMP-9, NFATC1 and c-Fos have been reported to play a pivotal role in osteoclast differentiation [26]. Therefore, we examined the effect of IL-29 on the expression of above genes by RT-real time PCR. In response to RANKL (50 ng/ml) treatment for 5 days, mRNA levels of TRAP, CTSK, MMP-9, NFATC1 and c-Fos in the RAW264.7 cells were dramatically increased when compared to that in unstimulated cells. However, this increase was dose-dependently inhibited by IL-29 (Fig. 4), suggesting that IL-29 may inhibit osteoclast differentiation through the inhibition of RANKL-induced TRAP, CTSK, MMP-9, NFATc1 and c-Fos expression.

3.5. IL-28Rα knockdown prevented IL-29 inhibition of RAW264.7 cell osteoclastogenesis

To further confirm the effect of IL-29 on osteoclast differentiation, RAW264.7 cells were transfected with scrambled shRNA controls and adenovirus vectors encoding shRNA against mouse IL-28Rα, then stimulated with IL-29 (100 ng/ml) and RANKL (50 ng/ml) for 5 days. IL-28Rα knockdown had no effect on the numbers of osteoclasts in unstimulated conditions but clearly prevented the inhibition of IL-29 in RANKL-induced osteoclast formation assessed by TRAP staining (Fig. 5). These data confirm that IL-29 suppresses osteoclastogenesis by directly inhibiting the differentiation of macrophages into osteoclasts.

3.6. Effects of IL-29 on RANKL-induced MAPK and STAT activation in osteoclasts

RANKL induced the activation of MAPK signaling pathway in osteoclast precursors is crucial for osteoclast differentiation [26], we next examined whether IL-29 affected MAPK pathway (p38, ERK and JNK) during osteoclast differentiation. RAW264.7 cells were treated with RANKL (50 ng/ml) in the presence or absence of IL-29 (100 ng/ml) for 8 min, 15 min and 30 min. The activation of MAPK was detected by Western blot in whole cell lysis. Result showed that JNK was markedly activated (phosphorylated) by RANKL at 8 min, and this activation was inhibited by IL-29 (Fig. 6). No effect of IL-29 on the activation (phosphorylation) of p38 and ERK was observed (Fig. 6).

It is widely accepted that IL-29 signals through the receptor complex and activates JAK-STAT pathway to induce antiviral, antitumor and other activities [2,11]. In this study, similarly, IL-29 (100 ng/ml) stimulated the activation of Stat1 (Tyr701) and Stat3 (Tyr705) in RAW264.7 (Fig. 6). No change in activation of Stat6 (Tyr641) was observed, and activation of Stat2 (Tyr690), Stat4 (Tyr693) and Stat5 (Tyr694) was not detectable in RAW264.7 cells. The results suggest that IL-29 may signal the cell through activation of the transcription factor Stat1 and 3 to inhibit osteoclast formation. Furthermore, we employed Stat1-specific inhibitor Fludarabine (50 μM) and Stat3-specific inhibitor Niclosamide (1 μM) to examine the role of Stat1 & 3 in IL-29-mediated osteoclastogenesis. As expected, the suppressive effect of IL-29 on osteoclast formation was abrogated by Fludarabine or Niclosamide (Supplementary Fig. 1). Osteoclasts were much more in Fludarabine or Niclosamide treated cells than those in the IL-29 treated cells, indicating that the IL-29 inhibitory action is associated with Stat1 & 3 pathways.

Supplementary data associated with this article can be found, in the online version, at https://doi.org/10.1016/j.cyto.2018.06.032.

3.7. Effects of IL-29 on RANKL-induced nucleartranslocation and expression of NF-κB and NFATc1

Activation of NF-κB is important in the activation and survival of mature osteoclasts, as well as osteoclastogenesis [27] and NFATc1 is one of the key transcription factors involved in osteoclast differentiation which is dependent upon NF-κB activation [26]. NFATc1 is retained in the cytoplasm in the inactive state and translocated into the nucleus after being activated. Therefore, we performed Western blot to analyze NF-κB-p65 and NFATc1in nuclear extracts (NEs) and cytoplasmic extracts (CEs). The data showed that NF-κB-p65 and NFATc1 in NEs dramatically increased after 48 h treatment by RANKL. However, NF-κB-p65 and NFATc1 nuclear translocation is inhibited by IL-29 (Fig. 7A), suggesting that IL-29 suppressed RANKL-induced NF-κB-p65

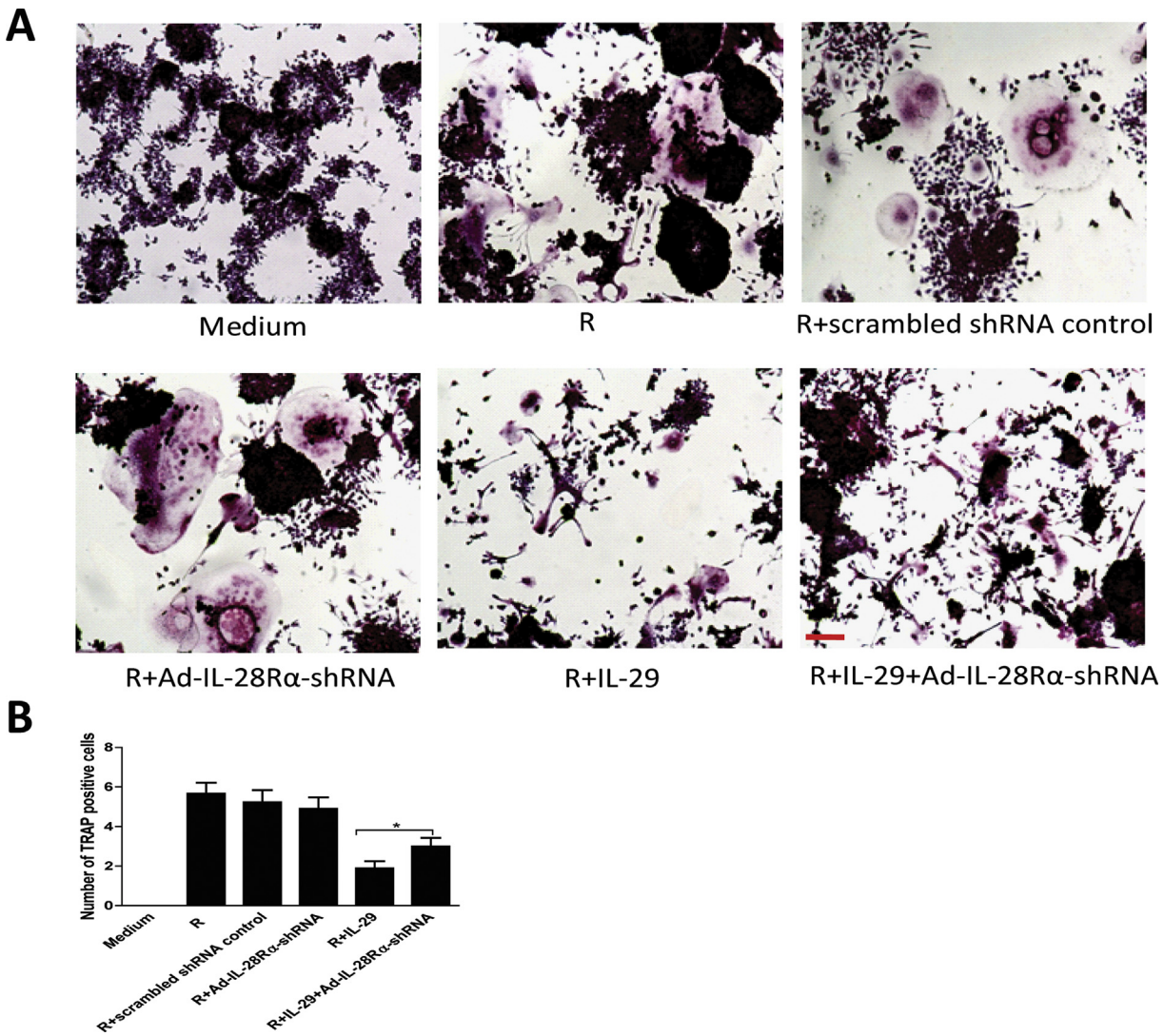

Fig. 5. IL-28Rα knockdown prevented IL-29 inhibition of RAW264.7 cell osteoclastogenesis. Cells were transfected with scrambled shRNA control and adenovirus vectors encoding shRNAs against mouse IL-28Rα (Ad-IL-28Rα-shRNA) for 48 h and further cultured with RANKL (50 ng/ml) and IL-29 (100 ng/ml) for 5 days, cells were then stained with TRAP. Scale bar: 50 μM. Statistics results were expressed as mean ± SEM (n = 3). $^{*}P < 0.05$ vs IL-29-treated group. R: RANKL. Medium: medium used for RAW264.7 cells treatment.

and NFATc1 nuclear translocation and activation during osteoclastogenesis in RAW264.7 cells. To confirm this function of IL-29, immunofluorescent staining and flow cytometric analysis were formed to examine the NFATc1 nuclear translocation. As shown in Fig. 7B, nuclear accumulation of NFATc1 was markedly increased by RANKL stimulation for 48 h compared with the non-treated cells, and these elevated levels of nuclear NFATc1 were clearly reduced by IL-29 (Fig. 7B). Similarly, the flow cytometric data confirmed that RANKL-induced NFATc1in NEs was significantly inhibited by IL-29 in RAW264.7 cells (Fig. 7C and D).

Furthermore, we investigated if there was a shorter window of IL-29 inhibition effect on NF-κB-p65 nuclear translocation and IκBα activation in RANKL-induced signaling. RAW264.7 cells were stimulated with IL-29 for 15, 30 and 60 min in the presence of RANKL as described above. IL-29 significant suppressed the activation of IκBα at 30 min and NF-κB-p65 nuclear translocation at 60 min (Supplementary Fig. 2B–E). Thus, our data suggest that IL-29 contributes to RANKL-induced nucleartranslocation and expression of NF-κB.

4. Discussion

In this study, we demonstrated, for first time that IL-29 inhibited RANKL-stimulated osteoclast activity and formation *in vitro*, implying the regulatory role of IL-29 on bone metabolism.

A delicate balance between bone resorption and bone formation is critical for the maintenance of bone metabolism, wherein bone-resorbing osteoclasts and bone-forming osteoblasts play central roles [28]. Osteoclasts are the only cells capable of resorbing bone in the body. In this study, we found that IL-29 inhibited RANKL-induced osteoclast formation (Fig. 2) and the resorptive activity of osteoclasts (Fig. 3) via its specific receptor IL-28Rα.

The role of IFNs in osteoclastogenesis has been well documented in many studies [18,28,29]. For example, IFN-γ strongly suppresses osteoclastogenesis *in vitro* [29]; conversely, it enhances osteoclast formation in cultures of peripheral blood from osteopetrotic patients, and induces human macrophages differentiation into osteoclasts [30,31]. IFN-β also inhibits the osteoclast differentiation [28] and exogenous IFN-β reduced bone destruction on a collagen antibody-induced arthritis model in mice via inhibiting the RANKL-c-Fos signaling pathway [32]. Similarly, IL-29 also showed the anti-osteoclastogenic effect *in*

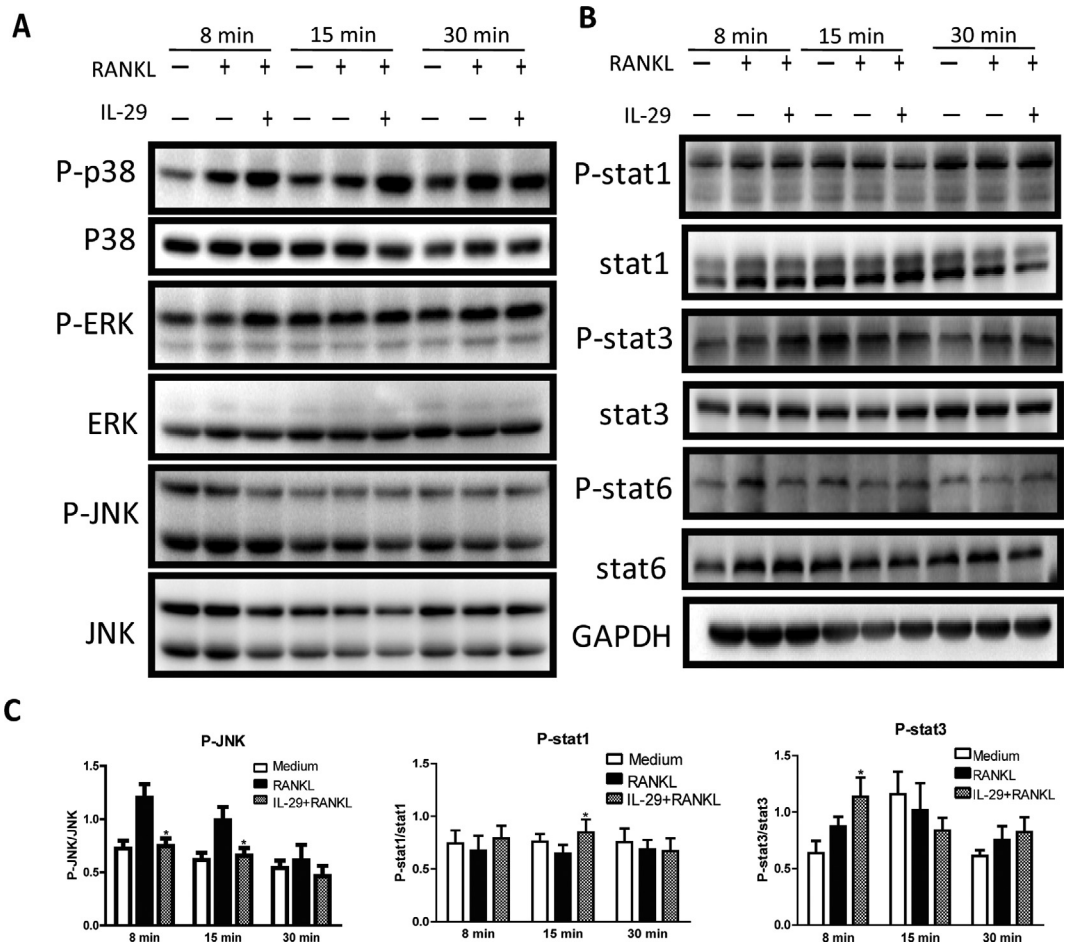

Fig. 6. Effects of IL-29 on the activation of MAPKs and JAK-STATs in RAW264.7 cells. The activation of JNK, ERK, P38, and STAT 1, 3, 6 in RAW264.7 cells treated with 100 ng/ml IL-29 in the presence of RANKL (50 ng/ml) stimulation for 8, 15 or 30 min, evaluated by western blot. The relative quantification of target proteins was calculated by comparison of the bands density levels between phosphorylated (P) and non-phosphorylated proteins. Results were expressed as mean ± SEM (n = 3). Images are a representative result of three independent experiments. $^{*}P < 0.05$ vs RANKL-treated group.

vitro via down-regulation of NF-κB and NFATc1 translocation in current study, which is beyond its original role in the immune responses. This effect of IL-29 may offer a molecular basis for the potential treatment of bone diseases.

RANKL binding to its receptor RANK on the surface of osteoclast precursor activates a series of intracellular signaling pathways including JNK, ERK, p38 MAPK and downstream molecules, including NF-κB, C-Fos and NFATc1 [33]. NF-κB pathway is the most important among RANKL-induced early signaling pathways [27]. When activated, NF-κB translocates into the nucleus where it enhances the expression of osteoclast-associated transcription factors. These factors, together with NF-κB stimulate the expression of genes essential for osteoclastogenesis such as TRAP, CTSK and MMP-9 and regulate osteoclast differentiation, function and survival. In this study, we found that IL-29 not only decreased the activation of JNK, but also suppressed c-Fos and NFATC1 expression, and NF-κB-p65 and NFATc1 nuclear transportation in RANKL-stimulated RAW264.7 cells (Figs. 4 and 7), resulting in down-regulation of NFATc1-mediated osteoclastogenic genes TRAP, CTSK and MMP-9 (Fig. 4), the latter were matrix enzymes contributing to degrade the bone matrix. In addition, IL-29 activated the transcription factor Stat1 and 3 in JAK-stat signaling pathway. Similarly, IFN-γ has been shown to inhibit RANKL-induced activation of NF-κB and JNK in BMMs [28] and suppress osteoclast formation through activation of Stat1 as this inhibitory effect of IFN-γ was completely abrogated in IFN-γR$^{-/-}$ and Stat1$^{-/-}$ mice [34]. IFN-β and IFN-α can also activation of Stat1 and 2, and this action was abrogated in BMMs from mice lacking Stat1 [34,35].

Our recent data indicates that IL-29 is an inflammatory cytokine and induces RANKL expression in synovial fibroblasts [5,17,36], however, the effect of IL-29 on RANKL expression is minimal. These results suggest that, similar to the action of type I and type II IFNs in RA [22], the anti-osteoclastogenic effects of IL-29 may outweigh its proinflammatory action although this hypothesis needs further investigation.

5. Conclusions

Collectively, our study presents the first evidence that IL-29 inhibits RANKL-induced osteoclast differentiation and function *in vitro*. Our results reveal a new biological function of IL-29 and may provide a molecular target for the treatment of bone diseases.

Acknowledgements

This project was sponsored by the grants from the National Natural Science Foundation of China (No. 81671610, 81471610, 81471611); the Priority Academic Program Development of Jiangsu Higher Education Institutions (PAPD). Dr. Xiangqing KONG is a Fellow at the Collaborative Innovation Center for Cardiovascular Disease Translational Medicine.

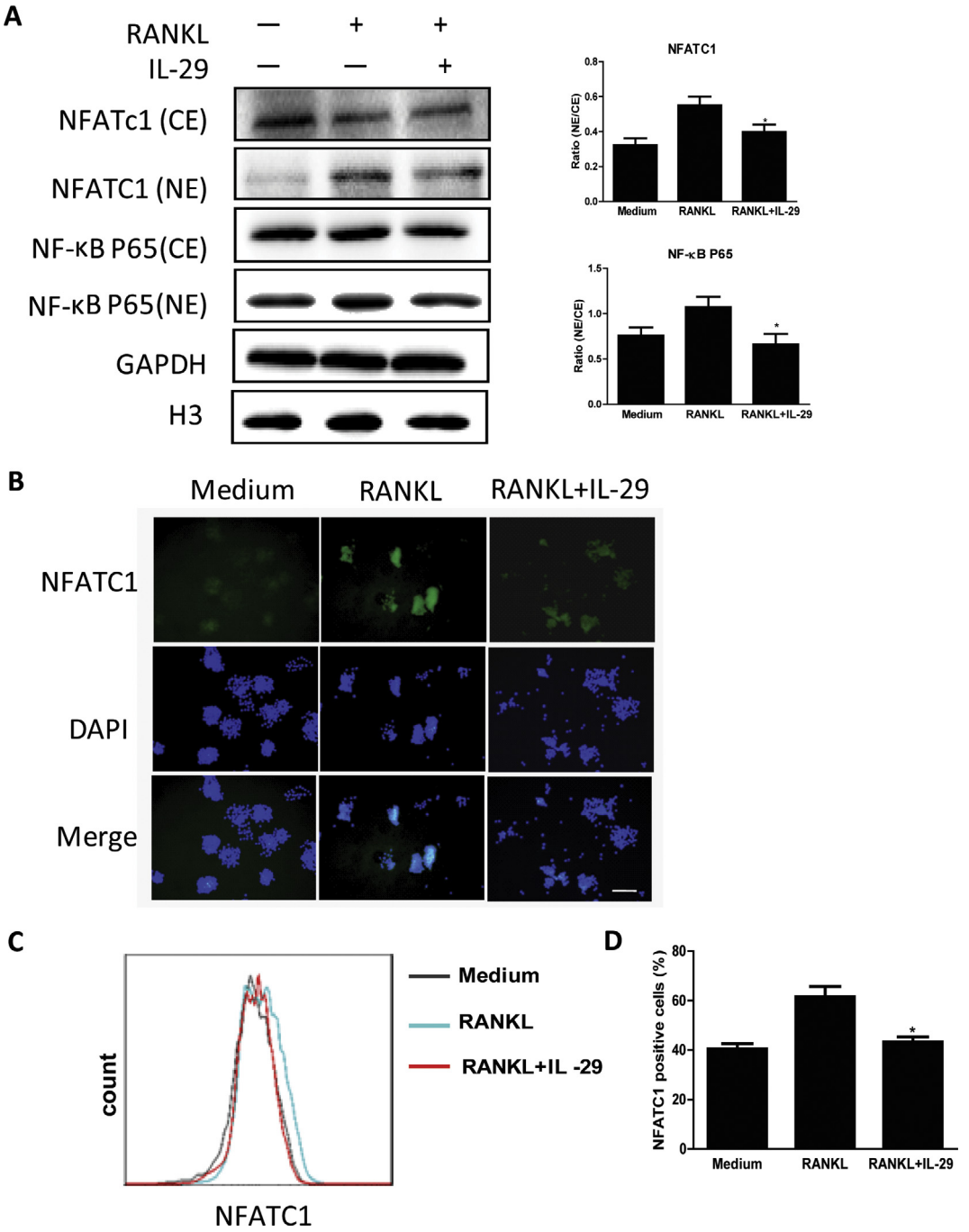

Fig. 7. Effects of IL-29 on RANKL-induced nuclear translocation of NF-κB-p65 and NFATc1. RAW264.7 cells were stimulated with RANKL (50 ng/ml) for 48 h in the absence or presence of IL-29 (100 ng/ml). (A) CEs and NEs, analyzed by western blot. Equal amounts of protein were loaded in each lane as demonstrated by the level of H3 (NE) and GAPDH (CE). (B) NFATc1, analyzed by immunofluorescent method. NFATc1: green; DAPI: blue. The nuclear localization ofNFATc1 was detected in merged images (cyan). (C&D) Cells were fixed and permeabilized and then analyzed on a FACSCalibur Flow cytometer. Images represent one of three independent experiments (C) and Data are expressed as mean ± SEM (n = 3) (D). Scale bar: 50 μM. $^{*}P < 0.05$ vs RANKL-treated group. Medium: medium used for RAW264.7 cells treatment.

Authors contributions

FW and WF conceived the study design, data analysis, and interpretation and the paper draft. QY, WH and QW carried out the cell culture. MQ, ZZ, AL and LX contributed to the immunoassay and flow cytometry. XQ, MJ and ML helped to edit the paper.

References

[1] S.V. Kotenko, G. Gallagher, V.V. Baurin, A. Lewis-Antes, M. Shen, N.K. Shah, J.A. Langer, F. Sheikh, H. Dickensheets, R.P. Donnelly, IFN-lambdas mediate antiviral protection through a distinct class II cytokine receptor complex, Nat. Immunol. 4 (1) (2003) 69–77.

[2] R.P. Donnelly, S.V. Kotenko, Interferon-lambda: a new addition to an old family, J. Interferon Cytokine Res. 30 (8) (2010) 555–564.

[3] K. Witte, G. Gruetz, H.D. Volk, A.C. Looman, K. Asadullah, W. Sterry, R. Sabat, K. Wolk, Despite IFN-lambda receptor expression, blood immune cells, but not keratinocytes or melanocytes, have an impaired response to type III interferons: implications for therapeutic applications of these cytokines, Genes Immun. 10 (8) (2009) 702–714.

[4] N.E. Kelm, Z. Zhu, V.A. Ding, H. Xiao, M.R. Wakefield, Q. Bai, Y. Fang, The role of IL-29 in immunity and cancer, Crit. Rev. Oncol. Hematol. 106 (2016) 91–98.

[5] F. Wang, L. Xu, X. Feng, D. Guo, W. Tan, M. Zhang, Interleukin-29 modulates proinflammatory cytokine production in synovial inflammation of rheumatoid arthritis, Arthritis Res. Ther. 14 (5) (2012) R228.
[6] L. Xu, Q. Peng, W. Xuan, X. Feng, X. Kong, M. Zhang, W. Tan, M. Xue, F. Wang, Interleukin-29 enhances synovial inflammation and cartilage degradation in osteoarthritis, Mediators Inflamm. 2016 (2016) 9631510.
[7] N.J. Megjugorac, G.E. Gallagher, G. Gallagher, Modulation of human plasmacytoid DC function by IFN-lambda1 (IL-29), J. Leukoc. Biol. 86 (6) (2009) 1359–1363.
[8] A. Kelly, M.W. Robinson, G. Roche, C.A. Biron, C. O'Farrelly, E.J. Ryan, Immune cell profiling of IFN-lambda response shows pDCs express highest level of IFN-lambda R1 and are directly responsive via the JAK-STAT pathway, J. Interferon Cytokine Res. 36 (12) (2016) 671–680.
[9] R.A. de Groen, A. Boltjes, J. Hou, B.S. Liu, F. McPhee, J. Friborg, H.L. Janssen, A. Boonstra, IFN-lambda-mediated IL-12 production in macrophages induces IFN-gamma production in human NK cells, Eur. J. Immunol. 45 (1) (2015) 250–259.
[10] M. Li, X. Liu, Y. Zhou, S.B. Su, Interferon-lambdas: the modulators of antivirus, antitumor, and immune responses, J. Leukoc. Biol. 86 (1) (2009) 23–32.
[11] S.V. Kotenko, IFN-lambdas, Curr. Opin. Immunol. 23 (5) (2011) 583–590.
[12] H.C. Steen, A.M. Gamero, Interferon-lambda as a potential therapeutic agent in cancer treatment, J. Interferon Cytokine Res.: Off. J Int. Soc. Interferon Cytokine Res. 30 (8) (2010) 597–602.
[13] Q. Wu, Q. Yang, E. Lourenco, H. Sun, Y. Zhang, Interferon-lambda1 induces peripheral blood mononuclear cell-derived chemokines secretion in patients with systemic lupus erythematosus: its correlation with disease activity, Arthritis Res. Ther. 13 (3) (2011) R88.
[14] S.C. Lin, C.C. Kuo, J.T. Tsao, L.J. Lin, Profiling the expression of interleukin (IL)-28 and IL-28 receptor alpha in systemic lupus erythematosus patients, Eur. J. Clin. Invest. 42 (1) (2012) 61–69.
[15] K. Wolk, K. Witte, E. Witte, M. Raftery, G. Kokolakis, S. Philipp, G. Schonrich, K. Warszawska, S. Kirsch, S. Prosch, W. Sterry, H.D. Volk, R. Sabat, IL-29 is produced by T(H)17 cells and mediates the cutaneous antiviral competence in psoriasis, Sci. Transl. Med. 5 (204) (2013) 204ra129.
[16] E. Apostolou, E.K. Kapsogeorgou, O.D. Konsta, I. Giotakis, M.I. Saridaki, E. Andreakos, A.G. Tzioufas, Expression of type III interferons (IFNlambdas) and their receptor in Sjogren's syndrome, Clin. Exp. Immunol. 186 (3) (2016) 304–312.
[17] L. Xu, X. Feng, W. Tan, W. Gu, D. Guo, M. Zhang, F. Wang, IL-29 enhances Toll-like receptor-mediated IL-6 and IL-8 production by the synovial fibroblasts from rheumatoid arthritis patients, Arthritis Res. Ther. 15 (5) (2013) R170.
[18] H. Takayanagi, K. Ogasawara, S. Hida, T. Chiba, S. Murata, K. Sato, A. Takaoka, T. Yokochi, H. Oda, K. Tanaka, K. Nakamura, T. Taniguchi, T-cell-mediated regulation of osteoclastogenesis by signalling cross-talk between RANKL and IFN-gamma, Nature 408 (6812) (2000) 600–605.
[19] F. Arai, T. Miyamoto, O. Ohneda, T. Inada, T. Sudo, K. Brasel, T. Miyata, D.M. Anderson, T. Suda, Commitment and differentiation of osteoclast precursor cells by the sequential expression of c-Fms and receptor activator of nuclear factor kappaB (RANK) receptors, J. Exp. Med. 190 (12) (1999) 1741–1754.
[20] D.L. Lacey, E. Timms, H.L. Tan, M.J. Kelley, C.R. Dunstan, T. Burgess, R. Elliott, A. Colombero, G. Elliott, S. Scully, H. Hsu, J. Sullivan, N. Hawkins, E. Davy, C. Capparelli, A. Eli, Y.X. Qian, S. Kaufman, I. Sarosi, V. Shalhoub, G. Senaldi, J. Guo, J. Delaney, W.J. Boyle, Osteoprotegerin ligand is a cytokine that regulates osteoclast differentiation and activation, Cell 93 (2) (1998) 165–176.
[21] Y.Y. Kong, H. Yoshida, I. Sarosi, H.L. Tan, E. Timms, C. Capparelli, S. Morony, A.J. Oliveira-dos-Santos, G. Van, A. Itie, W. Khoo, A. Wakeham, C.R. Dunstan, D.L. Lacey, T.W. Mak, W.J. Boyle, J.M. Penninger, OPGL is a key regulator of osteoclastogenesis, lymphocyte development and lymph-node organogenesis, Nature 397 (6717) (1999) 315–323.
[22] G. Schett, E. Gravallese, Bone erosion in rheumatoid arthritis: mechanisms, diagnosis and treatment, Nat. Rev. Rheumatol. 8 (11) (2012) 656–664.
[23] H. Takayanagi, Osteoimmunology: shared mechanisms and crosstalk between the immune and bone systems, Nat. Rev. Immunol. 7 (4) (2007) 292–304.
[24] M.M. Zaiss, M. Kurowska-Stolarska, C. Bohm, R. Gary, C. Scholtysek, B. Stolarski, J. Reilly, S. Kerr, N.L. Millar, T. Kamradt, I.B. McInnes, P.G. Fallon, J.P. David, F.Y. Liew, G. Schett, IL-33 shifts the balance from osteoclast to alternatively activated macrophage differentiation and protects from TNF-alpha-mediated bone loss, J. Immunol. 186 (11) (2011) 6097–6105.
[25] J.M. Quinn, N.A. Sims, H. Saleh, D. Mirosa, K. Thompson, S. Bouralexis, E.C. Walker, T.J. Martin, M.T. Gillespie, IL-23 inhibits osteoclastogenesis indirectly through lymphocytes and is required for the maintenance of bone mass in mice, J. Immunol. 181 (8) (2008) 5720–5729.
[26] M. Asagiri, K. Sato, T. Usami, S. Ochi, H. Nishina, H. Yoshida, I. Morita, E.F. Wagner, T.W. Mak, E. Serfling, H. Takayanagi, Autoamplification of NFATc1 expression determines its essential role in bone homeostasis, J. Exp. Med. 202 (9) (2005) 1261–1269.
[27] T. Miyazaki, H. Katagiri, Y. Kanegae, H. Takayanagi, Y. Sawada, A. Yamamoto, M.P. Pando, T. Asano, I.M. Verma, H. Oda, K. Nakamura, S. Tanaka, Reciprocal role of ERK and NF-kappaB pathways in survival and activation of osteoclasts, J. Cell Biol. 148 (2) (2000) 333–342.
[28] H. Takayanagi, S. Kim, T. Taniguchi, Signaling crosstalk between RANKL and interferons in osteoclast differentiation, Arthritis Res. 4 (Suppl 3) (2002) S227–S232.
[29] Y. Gao, F. Grassi, M.R. Ryan, M. Terauchi, K. Page, X. Yang, M.N. Weitzmann, R. Pacifici, IFN-gamma stimulates osteoclast formation and bone loss in vivo via antigen-driven T cell activation, J. Clin. Invest. 117 (1) (2007) 122–132.
[30] P.R. Madyastha, S. Yang, W.L. Ries, L.L. Key Jr., IFN-gamma enhances osteoclast generation in cultures of peripheral blood from osteopetrotic patients and normalizes superoxide production, J. Interferon Cytokine Res.: Official J. Int. Soc. Interferon Cytokine Res. 20 (7) (2000) 645–652.
[31] S. Kotake, Y. Nanke, M. Mogi, M. Kawamoto, T. Furuya, T. Yago, T. Kobashigawa, A. Togari, N. Kamatani, IFN-gamma-producing human T cells directly induce osteoclastogenesis from human monocytes via the expression of RANKL, Eur. J. Immunol. 35 (11) (2005) 3353–3363.
[32] R. Zhao, N.N. Chen, X.W. Zhou, P. Miao, C.Y. Hu, L. Qian, Q.W. Yu, J.Y. Zhang, H. Nie, X.H. Chen, P. Li, R. Xu, L.B. Xiao, X. Zhang, J.R. Liu, D.Q. Zhang, Exogenous IFN-beta regulates the RANKL-c-Fos-IFN-beta signaling pathway in the collagen antibody-induced arthritis model, J. Transl. Med. 12 (2014) 330.
[33] H. Takayanagi, New developments in osteoimmunology, Nat. Rev. Rheumatol. 8 (11) (2012) 684–689.
[34] G.R. Stark, I.M. Kerr, B.R. Williams, R.H. Silverman, R.D. Schreiber, How cells respond to interferons, Annu. Rev. Biochem. 67 (1998) 227–264.
[35] T. Taniguchi, K. Ogasawara, A. Takaoka, N. Tanaka, IRF family of transcription factors as regulators of host defense, Annu. Rev. Immunol. 19 (2001) 623–655.
[36] L. Xu, X. Feng, Y. Shi, X. Wang, X. Kong, M. Zhang, M. Liu, W. Tan, F. Wang, Interleukin-29 induces receptor activator of NF-kappaB ligand expression in fibroblast-like synoviocytes via MAPK signaling pathways, Int. J. Rheum. Dis. 18 (8) (2015) 842–849.